INTERNATIONAL JOURNAL OF AUTOMOTIVE SCIENCE AND TECHNOLOGY

2022, VOL. 6, NO: 2, 178-188 www.ijastech.org e-ISSN: 2587-0963

Comparative analysis of full car model with driver using PID and LQR controllers

Mustafa Eroğlu[1*], Mehmet Akif Koç[2], Recep Kozan[1], and İsmail Esen[3]

0000-0002-1429-7656, 0000-0001-7461-9795, 0000-0001-8544-883X, 0000-0002-7853-1464

[1] *Mechanical Engineering Department, Faculty of Engineering, Sakarya University, Sakarya, 54187, Turkey*
[2] *Mechatronics Engineering Department, Faculty of Technology, Sakarya Applied Science University, Sakarya, 54187, Turkey*
[3] *Mechanical Engineering Department, Faculty of Engineering, Karabük University, Karabük, 78050, Turkey*

Abstract

In this study, an active suspension model is proposed to increase the driving safety and passenger comfort of the car, which is adversely affected by car-road interaction. In this context, the full car model with a driver is considered as eight degrees of freedom. All the motion equations of the car were determined by the Lagrangian method and converted into state-space forms. Then, these equations are solved precisely by using Euler's method in Matlab software. PID and LQR controllers are designed to reduce the vertical displacement of the passenger and the rotational movements of the car. In order to evaluate the performance of the designed controllers, two different road inputs and two different car speeds are taken into account. In the simulation results, the vertical displacement and acceleration values of the driver and the rotational movements of the car were examined. While the PID controller stands out in damping the displacement values at low speeds, the LQR controller is much more successful in other cases.

Keywords: Full car model, Active suspension control, Ride control, PID, LQR

Research Article

https://doi.org/10.30939/ijastech..1076443

Received 20.02.2022
Revised 16.05.2022
Accepted 30.05.2022

* Corresponding author

Mustafa Eroğlu

mustafaeroglu@sakarya.edu.tr

Address: Mechanical Engineering Department, Faculty of Engineering, Sakarya University, Sakarya, Turkey

Tel:+903122028653

1. Introduction

In general, suspension systems consist of springs, shock absorbers, and connection elements. Thanks to the suspension systems, the disruptive effects coming from the road through the wheels are transmitted to the car and are reduced by damping. Suspension systems in cars affect driving safety and especially passenger comfort. Therefore, the performance of the suspension systems of the vehicles is essential for the automotive industry. However, it is not possible to have both driving safety and passenger comfort with superior performance at the same time. In such cases, actuators that can apply linear force in the vertical direction are added to the suspension systems to provide the desired performance in both features. Such systems are called active suspension systems. In other words, suspension systems can be examined in three categories as passive, semi-active and active.

In the literature, quarter car [1–7], half car [8–10], and full car [11–13] models are generally used for the analysis of car suspension systems. Hanafi controlled the semi-active car suspension system using PID (Proportional-Integral-Derivative) controller [14]. On the other hand, Güçlü and Metin used fuzzy logic control to control the vibration of the light rail vehicle [15]. Özmen and Közkurt suggested modeling and simulation of a fuzzy logic supported car driver control system in order to reduce human errors and uneconomical driver habits in traffic [16]. Doğan et al. used a quarter car model to control the suspension system separately in the Matlab/Simulink environment using PID and fuzzy logic [17]. The PID type controller can be used alone or usually used with other controllers. Emam used a fuzzy self-tuning PID controller to control the suspension system using a quarter car model [18]. Eroğlu et al. performs the control of the quarter car and bridge interaction model by using a self-tuning fuzzy PID controller [19]. Paksoy et al. performed semi-active control of the full car model using self-tuning fuzzy logic using Mr damper [20].

Traditional PID and fuzzy logic controllers are generally used to control car suspension systems. Apart from these, some studies prefer controllers such as SMC (Sliding mode control), LQR (linear quadratic regulator), and adaptive neuro-fuzzy inference system (Anfis). In this context, Yağız and Yüksek realized the control of the car model with 4 degrees of freedom using the SMC [21]. Sever et al. performed vibration control to ensure driving comfort and safety in quarter car model with biodynamic driver model by using LQR controller [3]. LQR controllers have many uses outside the car suspension system. For example, Çakır and Bayraktar used

an LQR controller in the main battle tank to reduce the oscillations of weapons and control the tank's movements, such as yaws and rolls [22]. In another study, active suspension control of smart flexible cantilever beams was performed using LQR [23]. There are also studies in which many of the control applications given above are used simultaneously. For example, Gandhi et al. used PID, LQR, fuzzy logic, and Anfis to control the 4 degrees of freedom half-car model and compared them with each other [9]. In addition, there are studies on the quarter car model using the bee algorithm and particle swarm optimization in some studies [24,25].

Active suspension control is carried out to increase the driving safety and passenger comfort of the eight degrees of freedom full car model with the driver examined in this study. The performance of the controllers is evaluated by applying the disturbance of the road on which the car passed to the car by considering two different scenarios. In the first scenario, it is aimed to control the pitch movement of the car, while in the second scenario, it is aimed to control both the pitch movement and the roll movement. In addition, analyzes are carried out by considering two different car speeds, not taking the car speed constant. A simulation study of the effect of modeled PID and LQR controllers on full car dynamics is conducted and compared with each other. In addition, the RMS graphics of the results of the analyzes made at all speeds from 1 m/s to 100 m/s are also given. In this case, it is understood that while the PID controller is superior at some speeds of the car, the LQR controller is superior at some speeds. However, in general, it has been determined that the LQR controller is more efficient in damping the vertical displacement of the driver and the rotational movements of the car.

2. Full car modeling and system description

This section will examine the modeling of a full car with eight degrees of freedom and different road profiles affecting the car. As shown in Fig. 1, the car body, wheels, and only one passenger are taken into account in the full car model with eight degrees of freedom. While only the vertical movements of the passenger and wheels are taken into account, the pitch and roll movements of the car are also examined along with the vertical movement. Apart from these, the lateral and rotational movements are neglected. The parameters md, mc, and mw represent the driver mass, car mass and wheel mass, respectively. The parameters I_{cx}, and I_{cy} correspond to the mass moment of inertia around the roll and pitch axis, respectively. The parameters k_d and c_d represent the suspension spring and damping coefficient between the driver and the car. k_{w1}, k_{w2}, k_{w3}, and k_{w4} indicate the vertical suspension spring coefficient between the car and the wheels, whereas c_{w1}, c_{w2}, c_{w3}, and c_{w4} indicate the vertical suspension damping coefficient between the car and the wheels. k_{r1}, k_{r2}, k_{r3}, and k_{r4} represent the tire spring coefficients. r_d and r_c represent the vertical displacement of driver and car, respectively, while r_{w1}, r_{w2}, r_{w3}, and r_{w4} represent the vertical displacement of four wheels. Also, the roll and the pitch motion of the car are shown as Θ_{cx} and Θ_{cy}. r_1, r_2, r_3, and r_4 represent the road inputs of the full car model. F_1, F_2, F_3, and F_4 are the actuator forces between the car and the wheels that can provide vertical force when necessary. The distances a and b represent between front wheels and center of car mass and rear wheels, and center of car mass. Whereas c and d represent right wheels and center of car mass and left wheels and center of car mass, respectively. e and f indicate the distance between the driver and the center of the car. All given parameters of the full car with eight degrees of freedom are shown in Table 1.

Since the full car model has eight degrees of freedom, eight independent equations of motion are obtained using the Lagrangian method. Two different road inputs, case I and case II, are applied to the vehicle wheels. In case I, the front and rear wheels of the vehicle enter the bump at the same time, while in the case II, first the left front wheel and then the right front wheel enter the bump. After these assumptions the kinetic energy, potential energy and damping function of the car model shown in Fig. 1 are given in the equations below.

$$E_k = \frac{1}{2}\begin{bmatrix} m_d\dot{r}_{dz}^2 + m_c\dot{r}_{cz}^2 + I_{cx}\dot{\theta}_{cx}^2 + I_{cy}\dot{\theta}_{cy}^2 + m_w\dot{r}_{w1z}^2 \\ +m_w\dot{r}_{w2z}^2 + m_w\dot{r}_{w3z}^2 + m_w\dot{r}_{w4z}^2 \end{bmatrix} \tag{1}$$

$$E_p = \frac{1}{2}\begin{bmatrix} k_{dz}\left[r_{dz} - r_{cz} + \theta_{cy}e - \theta_{cx}f\right]^2 \\ +k_{w1}\left[r_{cz} - r_{w1z} - \theta_{cy}a - \theta_{cx}c\right]^2 \\ +k_{w2}\left[r_{cz} - r_{w2z} - \theta_{cy}a + \theta_{cx}d\right]^2 \\ +k_{w3}\left[r_{cz} - r_{w3z} + \theta_{cy}b - \theta_{cx}c\right]^2 \\ +k_{w4}\left[r_{cz} - r_{w4z} + \theta_{cy}b + \theta_{cx}d\right]^2 \\ +k_{r1}\left[r_{w1z} - r_1\right]^2 + k_{r2}\left[r_{w2z} - r_2\right]^2 \\ +k_{r3}\left[r_{w3z} - r_3\right]^2 + k_{r4}\left[r_{w4z} - r_4\right]^2 \end{bmatrix} \tag{2}$$

$$D = \frac{1}{2}\begin{bmatrix} c_{dz}\left[\dot{r}_{dz} - \dot{r}_{cz} + \dot{\theta}_{cy}e - \dot{\theta}_{cx}f\right]^2 \\ +c_{w1}\left[\dot{r}_{cz} - \dot{r}_{w1z} - \dot{\theta}_{cy}a - \dot{\theta}_{cx}c\right]^2 \\ +c_{w2}\left[\dot{r}_{cz} - \dot{r}_{w2z} - \dot{\theta}_{cy}a + \dot{\theta}_{cx}d\right]^2 \\ +c_{w3}\left[\dot{r}_{cz} - \dot{r}_{w3z} + \dot{\theta}_{cy}b - \dot{\theta}_{cx}c\right]^2 \\ +c_{w4}\left[\dot{r}_{cz} - \dot{r}_{w4z} + \dot{\theta}_{cy}b + \dot{\theta}_{cx}d\right]^2 \end{bmatrix} \tag{3}$$

The Lagrangian expression ($L=E_k-E_p$) is equal to the difference between the kinetic and potential energies given in Eq. 1 and Eq. 2 and can be written as follows.

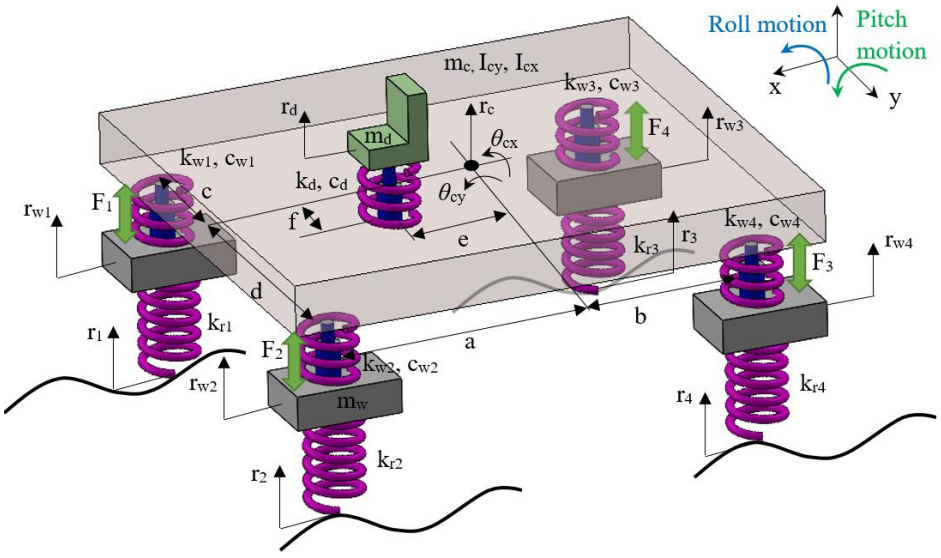

Fig 1. Physical model of full car model with driver

Table 1. Full car and road profile parameters

Full car model	
Driver mass (m_d)	100 kg
Car mass (m_c)	2000 kg
Wheel mass (m_w)	45 kg
Mass moment of inertia of car around pitch axis (Θ_{cy})	1500 kg.m^2
Mass moment of inertia of car around roll axis (Θ_{cx})	1680 kg.m^2
Primary suspension stiffness coefficient (k_d)	8000 N/m
Secondary suspension stiffness coefficient (k_{w1}, k_{w2}, k_{w3}, k_{w4})	25000 N/m
Tyre stiffness coefficient (k_{r1}, k_{r2}, k_{r3}, k_{r4})	150 kN/m
Primary suspension damping coefficient (c_d)	600 Ns/m
Secondary suspension damping coefficient (c_{w1}, c_{w2}, c_{w3}, c_{w4})	1000 Ns/m
Distance between front wheels and center of the car (a)	1.4 m
Distance between rear wheels and center of the car (b)	1.7 m
Distance between right wheels and center of the car (c)	0,75 m
Distance between left wheels and center of the car (d)	0.75 m
The vertical distance between driver and center of the car (e)	0.5 m
The lateral distance between driver and center of the car (f)	0.05 m
Road parameter	
Width of bump (a_1)	1 m
Distance between two successive bumps (a_2)	0.5 m
Height of bump (a_3)	0.1 m
Offset distance of bump (a_4)	0.75 m

$$\frac{\mathrm{d}}{\mathrm{d}t}\left(\frac{\partial L}{\partial \dot{\eta}_k(t)}\right)-\frac{\partial L}{\partial \eta_k(t)}+\frac{\partial D}{\partial \dot{\eta}_k(t)}=0\ ,\ k=1,2,3. \tag{4}$$

Generalized coordinates are given as in Eq. 5.

$$\boldsymbol{\eta}(t)=\left\{r_d\ r_c\ \theta_{cy}\ \theta_{cx}\ r_{w1}\ r_{w2}\ r_{w3}\ r_{w4}\right\}^T, \tag{5}$$

Eight equations of motion have been determined as follows, using the above.

For the driver seat's vertical displacement:

$$m_d\ddot{r}_d+k_d\left[r_d-r_c+\theta_{cy}e-\theta_{cx}f\right]+c_d\left[\dot{r}_d-\dot{r}_c+\dot{\theta}_{cy}e-\dot{\theta}_{cx}f\right]=0 \tag{6}$$

For the car's vertical displacement:

$$\begin{aligned}&m_c\ddot{r}_c-k_d\left[r_d-r_c+\theta_{cy}e-\theta_{cx}f\right]\\&+k_{w1}\left[r_c-r_{w1}-\theta_{cy}a-\theta_{cx}c\right]+k_{w2}\left[r_c-r_{w2}-\theta_{cy}a+\theta_{cx}d\right]\\&+k_{w3}\left[r_c-r_{w3}+\theta_{cy}b-\theta_{cx}c\right]+k_{w4}\left[r_c-r_{w4}+\theta_{cy}b+\theta_{cx}d\right]\\&-c_d\left[\dot{r}_d-\dot{r}_c+\dot{\theta}_{cy}e-\dot{\theta}_{cx}f\right]+c_{w1}\left[\dot{r}_c-\dot{r}_{w1}-\dot{\theta}_{cy}a-\dot{\theta}_{cx}c\right]\\&+c_{w2}\left[\dot{r}_c-\dot{r}_{w2}-\dot{\theta}_{cy}a+\dot{\theta}_{cx}d\right]+c_{w3}\left[\dot{r}_c-\dot{r}_{w3}+\dot{\theta}_{cy}b-\dot{\theta}_{cx}c\right]\\&+c_{w4}\left[\dot{r}_c-\dot{r}_{w4}+\dot{\theta}_{cy}b+\dot{\theta}_{cx}d\right]-\left[F_1+F_2+F_3+F_4\right]=0\end{aligned} \tag{7}$$

For the car's pitch motion:

(4)

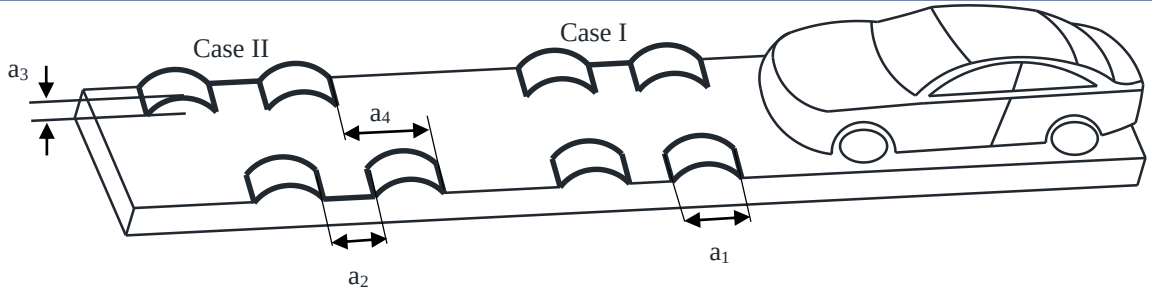

Fig 2. The road profile models

$$
\begin{aligned}
&I_{cy}\ddot{\theta}_{cy}+k_d e\left[r_d-r_c+\theta_{cy}e-\theta_{cx}f\right]\\
&-k_{w1}a\left[r_c-r_{w1}-\theta_{cy}a-\theta_{cx}c\right]-k_{w2}a\left[r_c-r_{w2}-\theta_{cy}a+\theta_{cx}d\right]\\
&+k_{w3}b\left[r_c-r_{w3}+\theta_{cy}b-\theta_{cx}c\right]+k_{w4}b\left[r_c-r_{w4}+\theta_{cy}b+\theta_{cx}d\right]\\
&+c_d e\left[\dot{r}_d-\dot{r}_c+\dot{\theta}_{cy}e-\dot{\theta}_{cx}f\right]-c_{w1}a\left[\dot{r}_c-\dot{r}_{w1}-\dot{\theta}_{cy}a-\dot{\theta}_{cx}c\right]\\
&-c_{w2}a\left[\dot{r}_c-\dot{r}_{w2}-\dot{\theta}_{cy}a+\dot{\theta}_{cx}d\right]+c_{w3}b\left[\dot{r}_c-\dot{r}_{w3}+\dot{\theta}_{cy}b-\dot{\theta}_{cx}c\right]\\
&+c_{w4}b\left[\dot{r}_c-\dot{r}_{w4}+\dot{\theta}_{cy}b+\dot{\theta}_{cx}d\right]+a\left[F_1+F_2\right]-b\left[F_3+F_4\right]=0
\end{aligned}
\tag{8}
$$

For the car's roll motion:

$$
\begin{aligned}
&I_{cx}\ddot{\theta}_{cx}-k_d f\left[r_d-r_c+\theta_{cy}e-\theta_{cx}f\right]\\
&-k_{w1}c\left[r_c-r_{w1}-\theta_{cy}a-\theta_{cx}c\right]+k_{w2}d\left[r_c-r_{w2}-\theta_{cy}a+\theta_{cx}d\right]\\
&-k_{w3}c\left[r_c-r_{w3}+\theta_{cy}b-\theta_{cx}c\right]+k_{w4}d\left[r_c-r_{w4}+\theta_{cy}b+\theta_{cx}d\right]\\
&-c_d f\left[\dot{r}_d-\dot{r}_c+\dot{\theta}_{cy}e-\dot{\theta}_{cx}f\right]-c_{w1}c\left[\dot{r}_c-\dot{r}_{w1}-\dot{\theta}_{cy}a-\dot{\theta}_{cx}c\right]\\
&+c_{w2}d\left[\dot{r}_c-\dot{r}_{w2z}-\dot{\theta}_{cy}a+\dot{\theta}_{cx}d\right]-c_{w3}c\left[\dot{r}_c-\dot{r}_{w3}+\dot{\theta}_{cy}b-\dot{\theta}_{cx}c\right]\\
&+c_{w4}d\left[\dot{r}_c-\dot{r}_{w4}+\dot{\theta}_{cy}b+\dot{\theta}_{cx}d\right]+c\left[F_1+F_3\right]-d\left[F_2+F_4\right]=0
\end{aligned}
\tag{9}
$$

For the vertical displacement of the first wheel:

$$
\begin{aligned}
&m_w\ddot{r}_{w1}-k_{w1}\left[r_c-r_{w1}-\theta_{cy}a-\theta_{cx}c\right]+k_{r1}\left[r_{w1}-r_1\right]\\
&-c_{w1}\left[\dot{r}_c-\dot{r}_{w1z}-\dot{\theta}_{cy}a-\dot{\theta}_{cx}c\right]+F_1=0
\end{aligned}
\tag{10}
$$

For the vertical displacement of the second wheel:

$$
\begin{aligned}
&m_w\ddot{r}_{w2}-k_{w2}\left[r_c-r_{w2}-\theta_{cy}a+\theta_{cx}d\right]+k_{r2}\left[r_{w2}-r_2\right]\\
&-c_{w2}\left[\dot{r}_c-\dot{r}_{w2}-\dot{\theta}_{cy}a+\dot{\theta}_{cx}d\right]+F_2=0
\end{aligned}
\tag{11}
$$

For the vertical displacement of the third wheel:

$$
\begin{aligned}
&m_w\ddot{r}_{w3}-k_{w3}\left[r_c-r_{w3}+\theta_{cy}b-\theta_{cx}c\right]+k_{r3}\left[r_{w3}-r_3\right]\\
&-c_{w3}\left[\dot{r}_c-\dot{r}_{w3}+\dot{\theta}_{cy}b-\dot{\theta}_{cx}c\right]+F_3=0
\end{aligned}
\tag{12}
$$

For the vertical displacement of the fourth wheel:

$$
\begin{aligned}
&m_w\ddot{r}_{w4}-k_{w4}\left[r_c-r_{w4}+\theta_{cy}b+\theta_{cx}d\right]+k_{r4}\left[r_{w4}-r_4\right]\\
&-c_{w4}\left[\dot{r}_c-\dot{r}_{w4}+\dot{\theta}_{cy}b+\dot{\theta}_{cx}d\right]+F_4=0
\end{aligned}
\tag{13}
$$

In this study, eight second-order differential equations belonging to the full car are obtained. These equations are reduced to 16 first-order differential equations with the help of state-space forms. Then Euler's method is used to solve these equations. The dynamic responses of the full car while passing through the road with different geometric shapes are analyzed with the commercial analysis program MATLAB. The necessary parameters for the car and road for the analysis are given in Table 1.

In this study, an active suspension system is used to increase passenger comfort, which is adversely affected by road disturbances. The road defects that adversely affect the car can be in different geometric shapes. In this study, as seen in Fig. 2, two different road disturbances are added to the system as inputs. In addition, four successive bump inputs are taken into account in both cases.

3. Controller Design

In this section, the controller design will be introduced, reducing the vibrations that negatively affect the car and the passenger in case of different speeds and disruptive road inputs. An active suspension system is obtained by adding an actuator that can create the vertical force to the suspension system of the full car model. Actuator force is shown with the symbol *F* in the full car's motion equations, and four controller forces will be obtained.

3.1 PID Controller Design

PID (Proportional-Integral-Derivative) controller is the most widely used type of controller in the literature, and its implementation is quite simple. The PID controller obtains a controller output by using the error signal of the system, as shown in Fig. 3. The error signals in this study are given in the following equation.

$$
\begin{aligned}
E_1(t)&=0-\left(r_c(t)-\theta_{cy}(t)a-\theta_{cx}(t)c\right)\\
E_2(t)&=0-\left(r_c(t)-\theta_{cy}(t)a+\theta_{cx}(t)d\right)\\
E_3(t)&=0-\left(r_c(t)+\theta_{cy}(t)b-\theta_{cx}(t)c\right)\\
E_4(t)&=0-\left(r_c(t)+\theta_{cy}(t)b+\theta_{cx}(t)d\right)
\end{aligned}
\tag{14}
$$

Each controller force can be determined separately using the error signals above as in the equation below.

$$F_i = k_p E_i(t) + k_i \int_0^t E_i(t)dt + k_d \frac{dE_i(t)}{dt} \qquad \text{i=1,2,3,4.} \qquad (15)$$

In the above equation, the coefficients k_p, k_i, and k_d represent the proportional gain, integral gain, and derivative gain of the PID controller. There are several methods for determining PID controller coefficients. The most preferred of these methods is the Ziegler-Nichols method. In this study, the parameters k_p=5*10^4 k_i=1*10^4 k_d=9*10^2 were chosen to provide the desired settling time and short rising time.

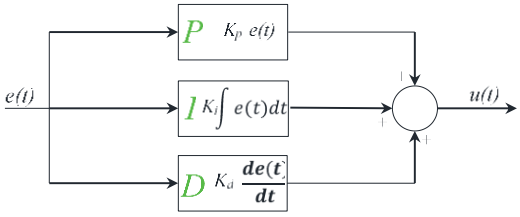

Fig 3. Controller design of PID

In the above equation, J defines the cost function, while Q and R define the matrices determined to reduce the cost function. Here, Q is a positive semi-definite matrix, and R is a positive definite matrix. The feedback control signal is defined as in Eq. 18. Here K is the state feedback gain matrix and can be determined as in Eq. 19. The P matrix is obtained using the algebraic Riccati equation shown in Eq. 20.

$$F(t) = -Kx \qquad (18)$$

$$K = R^{-1}B^T P \qquad (19)$$

$$PA + A^T P - PBR^{-1}B^T P = 0 \qquad (20)$$

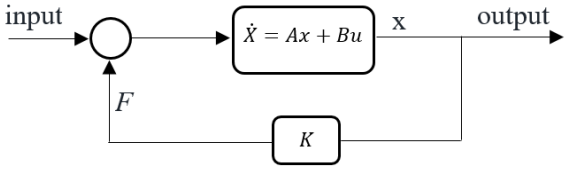

Fig 4. Controller design of LQR

3.2 LQR Controller Design

The primary purpose of LQR control, which is an optimal control theory, is to control dynamic systems with a minimum cost function. The cost function can be written as in Eq. 17 [23]. In LQR control, after the equations of motion of the full car model are converted to state-space form as in Eq. 16, an output feedback control force is determined by using state variables as in Fig. 4.

$$\dot{x}(t) = Ax(t) + Bu(t) \qquad (16)$$

$$J = \tfrac{1}{2}\int_0^\infty \left(x^T Qx + u^T Ru\right)dt \qquad (17)$$

In this study, the K gain matrix was found using the MATLAB command [K=lqr(A,B,QR)]. Here, Q and R parameters are important in determining the feedback gain matrix. These parameters were found using Bryson's method given in Eq. 21. The Q and R matrices found are given in Eq. 22 and Eq. 23.

$$Q_{jj} = \frac{1}{x_{j,\max}^2}, \quad R_{ii} = \frac{1}{u_{j,\max}^2} \qquad \text{j=1,2,...,16.} \quad \text{i=1,2,3,4.} \qquad (21)$$

$$Q = 10^4 \begin{bmatrix} 167 & 0 & 0 & 0 & 0 & 0 & 0 & 0 & 0 & 0 & 0 & 0 & 0 & 0 & 0 & 0 \\ 0 & 3.7 & 0 & 0 & 0 & 0 & 0 & 0 & 0 & 0 & 0 & 0 & 0 & 0 & 0 & 0 \\ 0 & 0 & 614 & 0 & 0 & 0 & 0 & 0 & 0 & 0 & 0 & 0 & 0 & 0 & 0 & 0 \\ 0 & 0 & 0 & 9.5 & 0 & 0 & 0 & 0 & 0 & 0 & 0 & 0 & 0 & 0 & 0 & 0 \\ 0 & 0 & 0 & 0 & 2567 & 0 & 0 & 0 & 0 & 0 & 0 & 0 & 0 & 0 & 0 & 0 \\ 0 & 0 & 0 & 0 & 0 & 12 & 0 & 0 & 0 & 0 & 0 & 0 & 0 & 0 & 0 & 0 \\ 0 & 0 & 0 & 0 & 0 & 0 & 3971 & 0 & 0 & 0 & 0 & 0 & 0 & 0 & 0 & 0 \\ 0 & 0 & 0 & 0 & 0 & 0 & 0 & 82 & 0 & 0 & 0 & 0 & 0 & 0 & 0 & 0 \\ 0 & 0 & 0 & 0 & 0 & 0 & 0 & 0 & 114 & 0 & 0 & 0 & 0 & 0 & 0 & 0 \\ 0 & 0 & 0 & 0 & 0 & 0 & 0 & 0 & 0 & 0.15 & 0 & 0 & 0 & 0 & 0 & 0 \\ 0 & 0 & 0 & 0 & 0 & 0 & 0 & 0 & 0 & 0 & 541 & 0 & 0 & 0 & 0 & 0 \\ 0 & 0 & 0 & 0 & 0 & 0 & 0 & 0 & 0 & 0 & 0 & 0.054 & 0 & 0 & 0 & 0 \\ 0 & 0 & 0 & 0 & 0 & 0 & 0 & 0 & 0 & 0 & 0 & 0 & 98.35 & 0 & 0 & 0 \\ 0 & 0 & 0 & 0 & 0 & 0 & 0 & 0 & 0 & 0 & 0 & 0 & 0 & 0.15 & 0 & 0 \\ 0 & 0 & 0 & 0 & 0 & 0 & 0 & 0 & 0 & 0 & 0 & 0 & 0 & 0 & 643 & 0 \\ 0 & 0 & 0 & 0 & 0 & 0 & 0 & 0 & 0 & 0 & 0 & 0 & 0 & 0 & 0 & 0.05 \end{bmatrix} \qquad (22)$$

$$R = 0.01\begin{bmatrix} 1 & 0 & 0 & 0 \\ 0 & 1 & 0 & 0 \\ 0 & 0 & 1 & 0 \\ 0 & 0 & 0 & 1 \end{bmatrix} \quad (23)$$

4. Simulation Results

In this study, the simulation results of the full car model with eight degrees of freedom are performed using Matlab software and by using different road profiles. The suspension parameters of the car to be controlled are given in Table 1. Accordingly, the control of the active suspension system was carried out using PID and LQR controllers in order to ensure passenger comfort and driving safety of the full car model.

The bumps were applied as disruptive road input to the car, and the vertical displacement of the driver and the rotational movements of the car were examined. In order to determine the performance of the designed controllers, two different paths, case I and case II, shown in Fig. 2, were defined as the system's input. Here, by applying Case I, it is desired to control the pitch movement of the car, while both pitch and roll movements are controlled by applying Case II. In addition, the performance of the two different controllers used was compared with each other using two different speeds, 25 m/s, and 50 m/s.

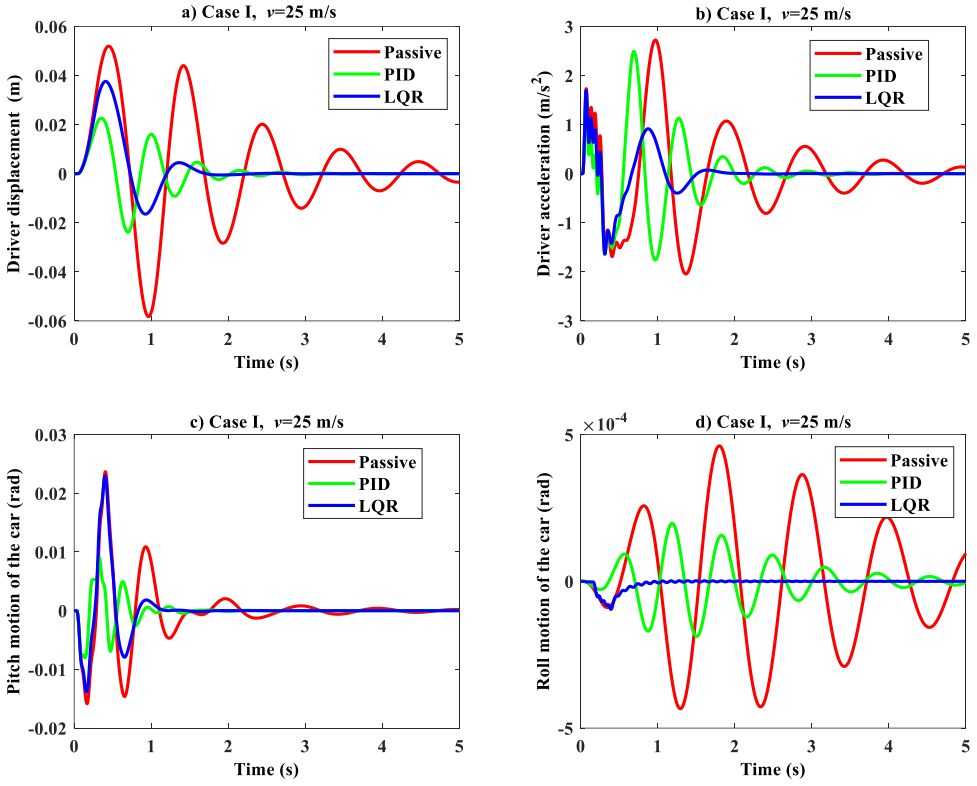

Fig 5. Time histories of the driver and car dynamic responses for the case I and *v*=25m/s

In Figs. 5 and 6, the effects on the driver of the car moving at 25 m/s and 50 m/s and the rotational movements of the car are analyzed. According to the graphics, it is seen that both controllers perform quite well compared to the passive suspension system. When the maximum vertical displacement of the driver is examined, it is seen that while it is 0.058 m in the case of the passive suspension system, it is 0.023 m and 0.037 m in the case of PID and LQR controllers, respectively. In this case, it is seen that the PID controllers perform better on the vertical displacement of the driver, but the LQR controller also dampens the oscillations in a shorter time. In Fig. 5b, it is clearly seen that the LQR controller is relatively superior to the passive and PID controller. According to the pitch and roll motion graphics of the car in Figs. 5c and 5d, it is seen that the PID controller reduces the pitch motion, while the LQR controller also reduces the roll motion. In Fig. 6, the car speed of 50 m/s is given for case I. Although the graphics in Fig. 6 are quite similar to those in Fig. 5, it has been observed that the performance of the LQR controller increases more than the PID controller as the speed increases

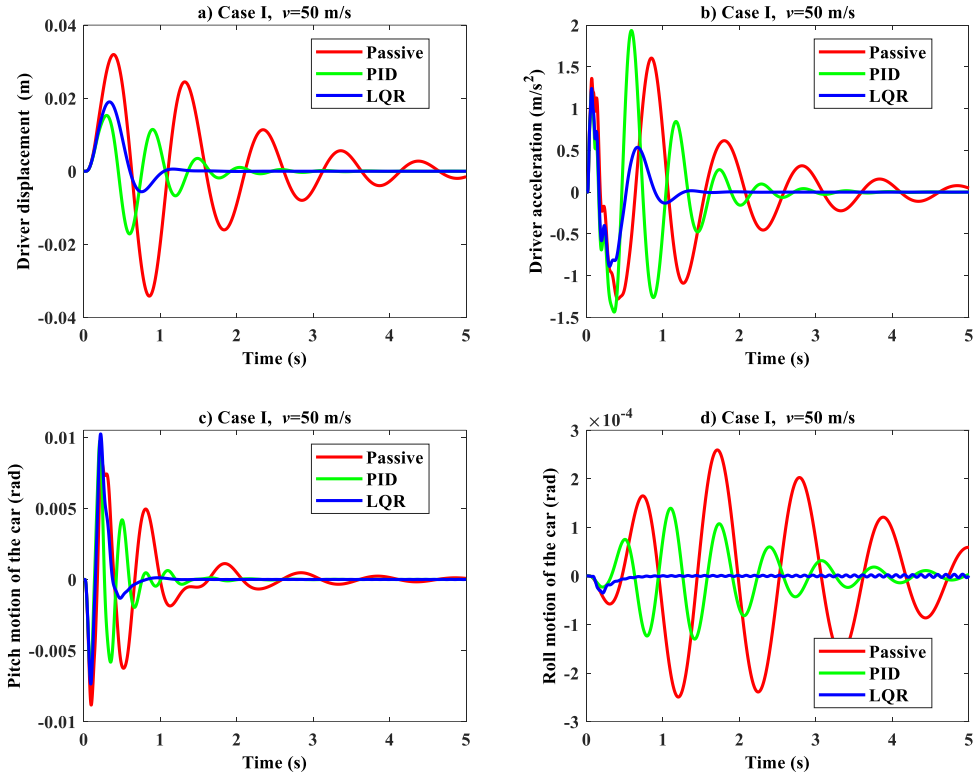

Fig 6. Time histories of the driver and car dynamic responses for the case I and *v*=50m/s

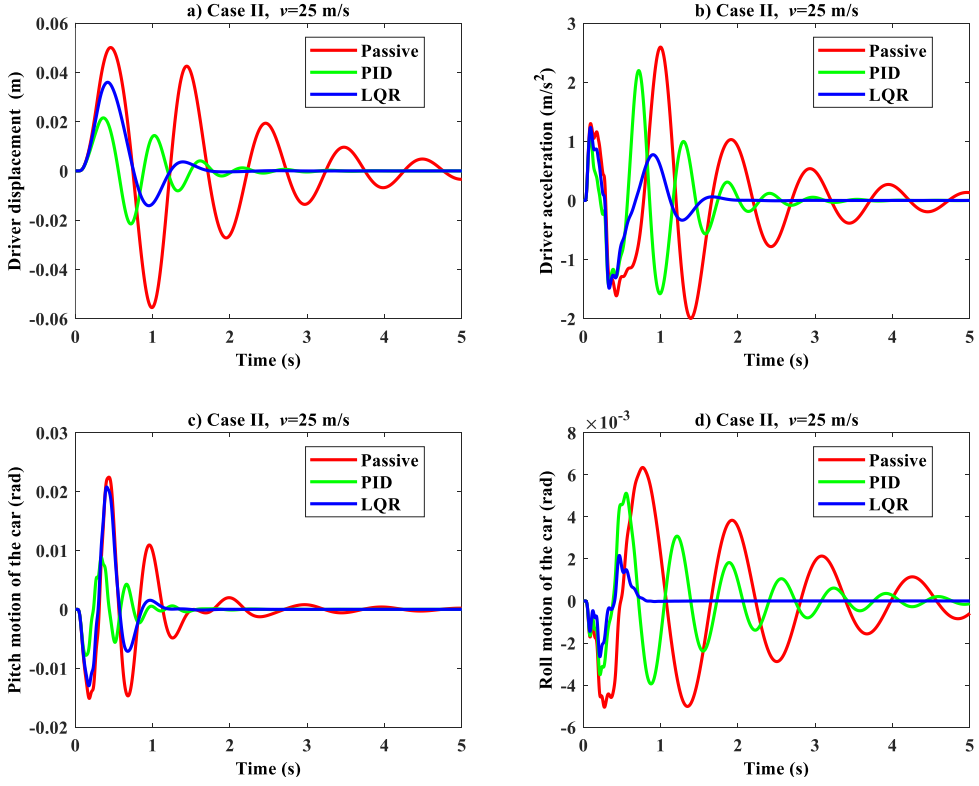

Fig 7. Time histories of the driver and car dynamic responses for the case II and *v*=25m/s

.

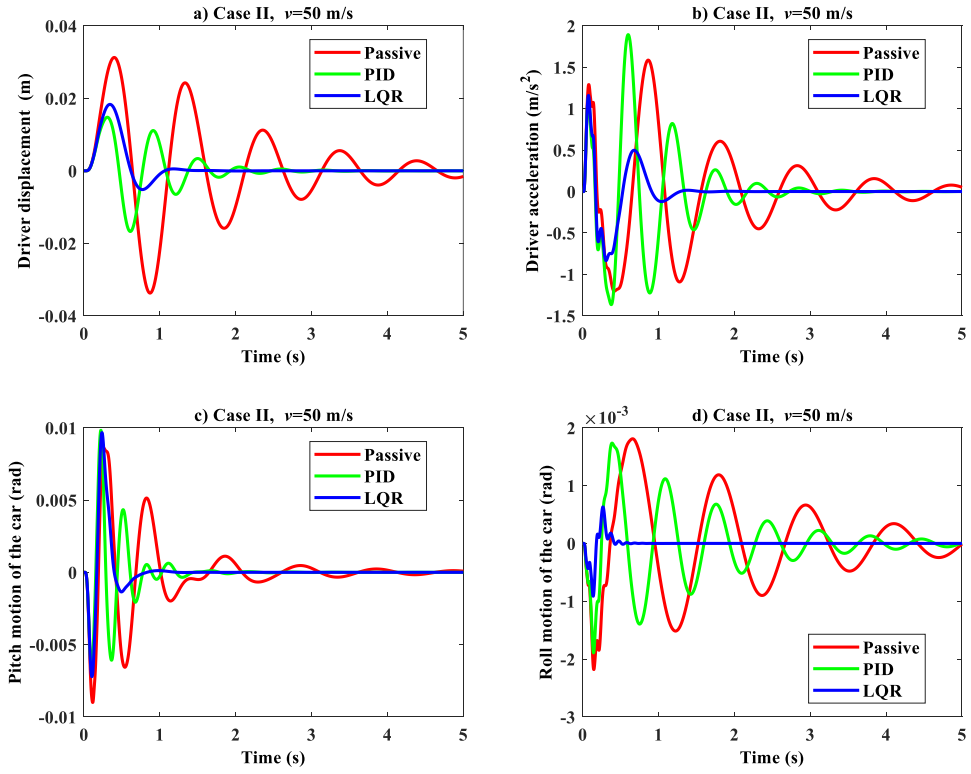

Fig 8. Time histories of the driver and car dynamic responses for the case II and *v*=50m/s time

In Figs. 7 and 8, dynamic behaviors of the driver and the car are given in case II road input. Similarly, while the PID controller is superior in damping vertical displacements, the LQR controller is superior in damping vertical accelerations. However, when Fig. 8b is examined, although the vertical displacement of the driver is less in the PID controller, it is understood that the LQR controller is more successful in this graph. In both Figs. 7b and 8b, it is seen that the LQR controller is more efficient in reducing the acceleration values than the PID controller.

When case I and case II road input are examined, it is understood that the roll motion of the car is quite different. For example, in Fig. 5d, the maximum roll motion of the car is 4.6x10-4 rad, while in Fig. 7, the roll motion of the car is 6.3x 10-3 rad. In other words, the roll motion of the car increases approximately 14 times. However, thanks to the active suspension controllers, the roll motion of the full car is considerably reduced and can be damped in a short time.

In Figs. 9a and 10a, the RMS values of the simulation results of the passive suspension and active suspension systems when the car speed changes from 1 m/s to 100 m/s in the range of 1 m/s are given. When the vertical displacement graphs of the driver in Figs. 9a and 10a are examined, it is seen that both controllers perform better than the passive suspension system. However, in both graphs, while the PID controller was superior up to the car's speed of about 40 m/s, the LQR controller was superior at car speeds above this speed. When the vertical acceleration values of the car are examined in Figs. 9b and 10b, it is seen that the LQR controller is more efficient at almost all speeds. The results in the graphs in Figs. 9c and 10c are quite similar to the results for vertical displacement of the driver. In these graphs, the LQR controller gives better results if the car speed is more than 40 m/s. When Figs. 9d and 10d are examined, it is understood that they are different from each other. This is because the case II road input forces the car to oscillate in the roll direction. In addition, in these graphs, the LQR controller dampens vibrations by reducing oscillations in a much shorter time than passive and PID controllers.

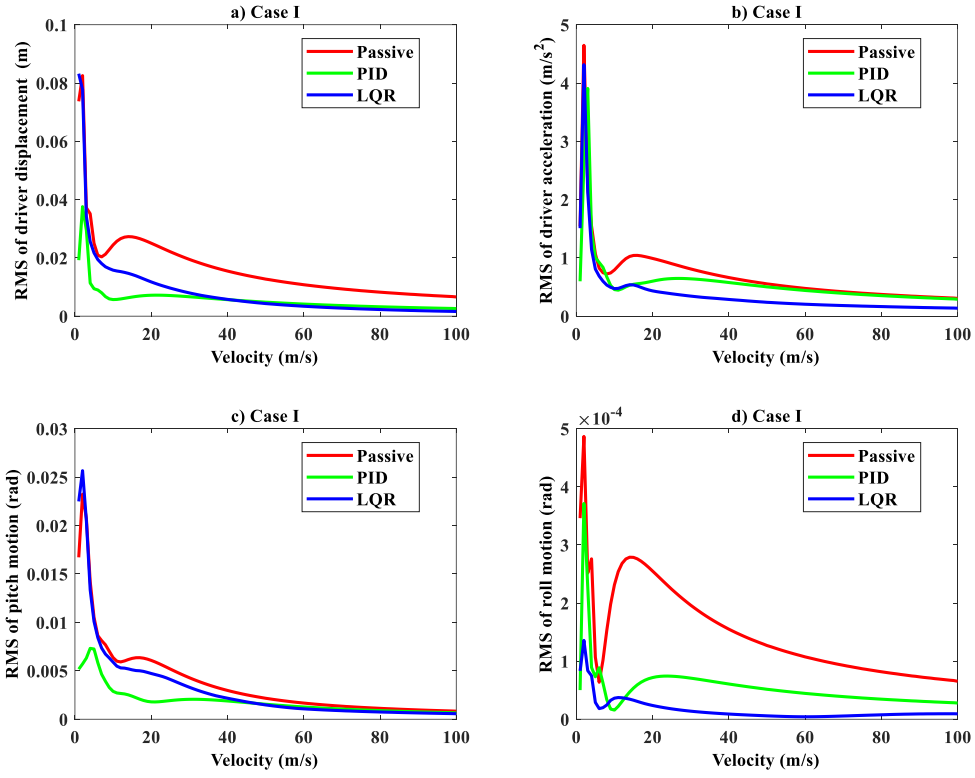

Fig 9. Time RMS of the driver and car dynamic responses for the case I

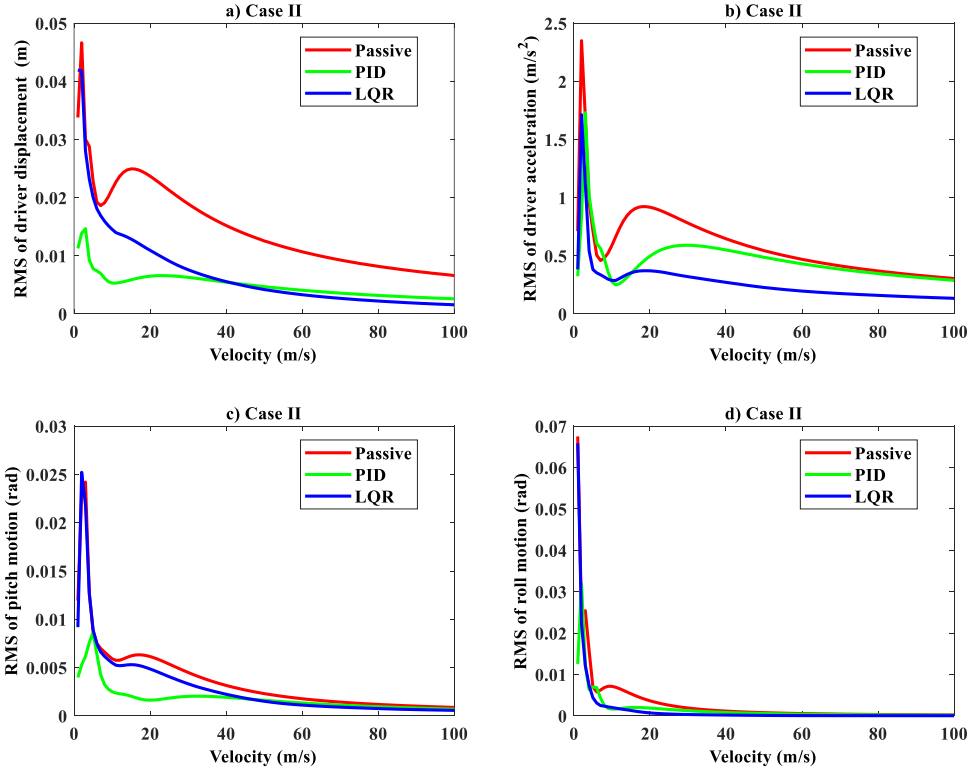

Fig 10. Time RMS of the driver and car dynamic responses for the case II

5. Conclusions

In this study, an active suspension system was designed to improve the road holding and passenger comfort of the car by using the full car model. The control of the active suspension system was carried out using conventional PID and LQR controllers. Matlab software was used to determine the dynamic behaviors of the full car model. The equations of motion of the car were obtained using the Lagrangian method, and the obtained equations of motion were converted into state-space form. The performances of the controllers were compared by considering two different disruptive effects from the road to the full car model, taking into account two different car speeds. According to the simulation results, the PID controller was more efficient in reducing the displacement and pitch movement of the car at low speeds. It has been seen that the LQR controller is more efficient in controlling the acceleration and roll motion of the car, regardless of car speed. In addition, when all graphics are examined, the oscillations of the car and the dynamic behavior of the car can be reduced much faster, especially at high speeds, thanks to the LQR controller.

Conflict of Interest Statement

The authors declare that there is no conflict of interest in the study.

CRediT Author Statement

Mustafa Eroğlu: Conceptualization, Software, Writing-original draft.
M. Akif Koç: Writing-Review, Supervision.
Recep Kozan: Writing-Review, Supervision.
İsmail Esen: Writing-Review, Supervision.

References

[1] Y. Altun, Çeyrek Taşıt Aktif Süspansiyon Sistemi için LQR ve LQI Denetleyicilerinin Karşılaştırılması, Gazi Üniversitesi Fen Bilim. Derg. Part C Tasarım ve Teknol. 2017;5:61–70. http://dergipark.gov.tr/http-gujsc-gazi-edu-tr/issue/31140/338335.

[2] M. Nagarkar, Y. Bhalerao, G.V. Patil, R.Z. Patil, Multi-Objective Optimization of Nonlinear Quarter Car Suspension System - PID and LQR Control, Procedia Manuf. 2018;20:420–427. doi:10.1016/j.promfg.2018.02.061.

[3] M. Sever, H.S. Şendur, H. Yazıcı, M.S. Arslan, Biodinamik sürücü modeli içeren bir taşıt süspansiyon sisteminin durum türevi geri beslemeli LQR ile aktif titreşim kontrolü, Gazi Üniversitesi Mühendislik-Mimarlık Fakültesi Derg.2019;3:1573–1572. doi:10.17341/gazimmfd.570732.

[4] M.E.H. Jamadar, R.M. Desai, H. Kumar, S. Joladarashi, Analyzing quarter car model with Magneto-Rheological (MR) damper using equivalent damping and Magic formula models, Mater. Today Proc. 2019;46: 9944–9949. doi:10.1016/j.matpr.2021.02.706.

[5] D. Singh, Active Vibration Control of Passenger Seat in Quarter Car Model using Supertwisting Controller, Int. J. Control Autom. 2017;10:83–94. doi:10.14257/ijca.2017.10.11.08.

[6] P.R. Nwagoum Tuwa, T. Molla, S. Noubissie, S.T. Kingni, K. Rajagopal, Analysis of a quarter car suspension based on a Kelvin–Voigt viscoelastic model with fractional-order derivative, Int. J. Non. Linear. Mech. 2021;137:103818. doi:10.1016/j.ijnonlinmec.2021.103818.

[7] H. Okuturlar, M. Tınkır, Araç süspansiyon sisteminin nümerik ve deneysel dinamik analizi, Konya J. Eng. Sci. 2021;9:85–105. doi:10.36306/konjes.778390.

[8] J.O. Pedro, S.M.S. Nhlapo, L.J. Mpanza, Model predictive control of half-car active suspension systems using particle swarm optimisation, IFAC-PapersOnLine. 2020;53:14438–14443. doi:10.1016/j.ifacol.2020.12.1443.

[9] P. Gandhi, S. Adarsh, K.I. Ramachandran, Performance Analysis of Half Car Suspension Model with 4 DOF using PID, LQR, FUZZY and ANFIS Controllers, Procedia Comput. Sci. 2017;115: 2–13. doi:10.1016/j.procs.2017.09.070.

[10] H. Khodadadi, H. Ghadiri, Self-tuning PID controller design using fuzzy logic for half car active suspension system, Int. J. Dyn. Control. 2018;6:224–232. doi:10.1007/s40435-016-0291-5.

[11] E. Yildirim, I. Esen, Dynamic Behavior and Force Analysis of the Full Vehicle Model using Newmark Average Acceleration Method, Eng. Technol. Appl. Sci. Res. 2020;10:5330–5339. doi:10.48084/etasr.3335.

[12] H. Jing, R. Wang, C. Li, J. Bao, Robust finite-frequency H∞ control of full-car active suspension, J. Sound Vib. 441 (2019) 221–239. doi:10.1016/j.jsv.2018.06.047.

[13] D. Ben Hassen, M. Miladi, M.S. Abbes, S.C. Baslamisli, F. Chaari, M. Haddar, Road profile estimation using the dynamic responses of the full vehicle model, Appl. Acoust. 2019;147:87–99. doi:10.1016/j.apacoust.2017.12.007.

[14] D. Hanafi, PID controller design for semi-active car suspension based on model from intelligent system identification, 2010 2nd Int. Conf. Comput. Eng. Appl. ICCEA 2010. 2 (2010) 60–63. doi:10.1109/ICCEA.2010.168.

[15] R. Guclu, M. Metin, Fuzzy logic control of vibrations of a light rail transport vehicle in use in Istanbul traffic, JVC/Journal Vib. Control. 2009;15:1423–1440. doi:10.1177/1077546309102664.

[16] İ. Özmen, C. Közkurt, Design of Fuzzy Logic Supported Car Driver Control System, Int. J. Automot. Sci. Technol. 2021;5: 228–238. doi:10.30939/ijastech..902139.

[17] H. Doğan, K. Kaplan, M. Kuncan, H.M. Ertunç, K. Üniversitesi, Araç Süspansiyon Sistemi Kontrolüne PID ve Bulanık Mantık Yaklaşımları PID and Fuzzy Logic Approach to Vehicle Suspension System Control Mekatronik Mühendisliği Bölümü.2015;10–12.

[18] A.S. Emam, Fuzzy Self Tuning of PID Controller for Active Suspension System, Adv. Powertrains Automotives. (2015). doi:10.12691/apa-1-1-4.

[19] M. Eroğlu, M.A. Koç, R. Kozan, İ. Esen, Self-tuning fuzzy logic control of quarter car and bridge interaction model, Sak. Univ. J. Sci. 25 (2021) 1197–1209. doi:10.16984/saufenbilder.863063.

[20] M. Paksoy, R. Guclu, S. Cetin, Semiactive self-tuning fuzzy logic control of full vehicle model with MR damper, Adv. Mech. Eng. 2014. doi:10.1155/2014/816813.

[21] N. Yağız, İ. Yüksek, Robust Control of Active Suspensions Using Sliding Modes, Env. Sci. 2001;25: 79–87.

[22]M.F. Cakir, M. Bayraktar, Modelling of main battle tank and designing LQR controller to decrease weapon oscillations, J. Fac. Eng. Archit. Gazi Univ.2020;35:1861–1876. doi:10.17341/gazimmfd.660584.

[23]K.G. Aktas, I. Esen, State-Space Modeling and Active Vibration Control of Smart Flexible Cantilever Beam with the Use of Finite Element Method, Eng. Technol. Appl. Sci. Res. 2020;10: 6549–6556. doi:10.48084/etasr.3949.

[24]O. Eser, A. Çakan, M. Kalyoncu, F. Botsalı, AriAlgoritmasi (AA) Ve Parçacik SürOptimizasyonu (PSO) Kullanarak Çeyrek AraçModeli TasariParametreleriniBelirlenmesi, Konya J. Eng. Sci. 8055.2021; 621–632. doi:10.36306/konjes.881062.

[25]R. Kothandaraman, L. Ponnusamy, PSO tuned Adaptive Neuro-fuzzy Controller for Vehicle Suspension Systems, J. Adv. Inf. Technol. 3 (2012) 57–63. doi:10.4304/jait.3.1.57-63.